branching fraction
Einstein A and B coefficients
channel!decay
absorption!oscillator strength
oscillator strength

17. Precision Oscillator Strength and Lifetime Measurements

The accuracy of oscillator strength and lifetime measurements has improved greatly in the past twenty years. Nevertheless, these high accuracies have been achieved for only a restricted number of lines belonging to a few elements and ionization stages [17.1]. Large numbers of precision measurements must still be made as improved experimental oscillator strengths are needed, both as tests of theoretical concepts, and for diagnostics and engineering applications.

A spectral line arising from a radiative transition between atomic states i and k is characterized by its wavelength λ_{ik}, its intensity and its shape. In the limit of free atoms, the intensity per atom is determined by the emission transition rate A_{ik} or absorption oscillator strength f_{ki}, and the shape by the natural width $\Gamma_i = \hbar/\tau_i$, where τ_i is the lifetime of the excited state. While classical spectroscopic methods provide precise wavelength measurements (1 part in 10^8 or better; Chapt. 10), it has only recently been possible to measure oscillator strengths and lifetimes to better than a few percent, as discussed in this chapter. Examples of applications which require an accurate knowledge of these quantities are the interpretation of astrophysical data (Chapt. 82), atmospheric physics (Chapt. 84), combustion (Chapt. 88), the modeling and diagnosis of thermonuclear plasmas (Chapt. 86), nonlinear optics (Chapt. 72), isotope separation (Chapt. 16), and the development of new types of lasers (Chapt. 71).

Precision measurements of oscillator strengths and lifetimes also provide stringent tests of atomic structure calculations. These quantities are very sensitive to the wave functions and the approximations used, particularly in cases where electron correlations (Sect. 23.2.1) and relativistic effects (Sect. 22.1) are significant. They provide experimental tests of fundamental theory; for example, of quantum electrodynamic corrections (Sect. 27.2), and of the nonconservation of parity predicted by the unified electro-weak theory (Sect. 29.1).

In applications where only modest precision is required, semi-empirical parameterizations involving quantum defects, charge screening and polarization allow a few precise measurements to be extrapolated along isoelectronic, homologous, isoionic and Rydberg sequences. Similar methods have been applied to the atomic energy levels themselves (Sect. 10.13). They allow one to produce a very large data base of moderate precision [17.2].

The spontaneous transition rate A_{ik} (Sect. 10.16.2) is the probability per unit time (s^{-1}) for an atom in any one of the g_i states of the energy level i to make a transition to any of the g_k states of the level k. The lifetime τ_i is then given by $1/\tau_i = \sum_k A_{ik}$. The branching fraction for the kth channel of the decay of level i is defined as $F_B = \tau_i A_{ik}$, and the branching ratio (Sect. 10.17) between two decay channels is $R_B = A_{ik}/A_{ij}$. Emission and absorption rate constants differ by a factor of λ_{ik}^2, and the absorption oscillator strength f_{ki} (Sect. 10.17) is defined by

$$g_k f_{ki} = C\lambda_{ik}^2 g_i A_{ik} \,, \qquad (17.1)$$

where $C = (32\pi^3 \alpha a_0^2 \mathrm{Ry})^{-1} = 1.499\,19 \times 10^{-14}\,\mathrm{nm}^{-2}\,\mathrm{s}$. Because of this relationship, the words transition rate and oscillator strength will be used almost interchangeably.

Springer Handbook
MS ID: **hb05-b17**
13 June 2005 10:35 CET

17.1 Oscillator Strengths

Oscillator strengths can be determined directly through absolute emission, absorption, or dispersion measurements, or through the combined measurement of branching ratios and lifetimes. Direct measurements compare different transitions at the same time, and require sample equilibrium, a knowledge of the absolute number density, and an absolute intensity measurement. These are in contrast to time-resolved lifetime measurements, which compare relative intensities from the same transition at different times, and require no absolute measurements. However, lifetime measurements yield oscillator strengths directly only in cases where a single decay transition channel exists, such as the lowest excited level in an atom or ion. Thus, combined measurements of lifetimes and branching ratios are often used where high precision values for oscillator strengths are required. Both absorption and dispersion measurements involve the number density of the lower level of the transition, whereas emission measurements involve that of the upper level.

17.1.1 Absorption and Dispersion Measurements

Absorption measurements involve placing a sample of atoms (for example, in a gas cell, an atomic beam, an arc, a shock tube, or within the vapor column in a furnace) between a continuous light source and a spectrometer. For an isolated spectral line, the absorption cross section for a beam of photons of frequency ν passing through the sample is

$$\sigma_{ik}(\nu) = \pi\alpha(\hbar/m)g(\nu)f_{ik}\,, \tag{17.2}$$

where $g(\nu)$ is the spectral distribution function per unit frequency normalized so that $\int_0^\infty g(\nu)\,\mathrm{d}\nu = 1$. If there are N atoms per unit volume, the absorption coefficient is $k_\nu = N\sigma(\nu)$. The integrated intensity lost after passing through a distance L of the sample is

$$\int_0^\infty \Delta I(\nu)\,\mathrm{d}\nu = I_0 \int_0^\infty \left(1 - \exp^{-\sigma_{ik}(\nu)NL}\right)\,\mathrm{d}\nu \simeq I_0\pi\alpha(\hbar/m)NL\,f_{ik}\,, \tag{17.3}$$

where the second line applies if the sample is optically thin. Otherwise, the integral can be calculated directly, if $g(\nu)$ is known, to determine f_{ik} by the curve-of-growth method.

The Furnace Method

High precision absorption measurements have been achieved by *Blackwell* and co-workers [17.3], who have used the furnace method to study the astrophysically important neutral iron spectrum. These measurements have quoted accuracies of 0.5% on a relative scale, and 2.5% on an absolute scale. This accuracy was obtained through the use of a stable and isothermal furnace, low-noise spectral intensity recording techniques, and two identical high resolution spectrometers for the simultaneous recording of pairs of absorption lines. By selecting successive line pairs of a suitable oscillator strength ratio and adjusting the temperature and vapor pressure in the furnace, a large dynamic range of oscillator strengths could be covered. Recently, corroborative studies of the uncertainties quoted in these measurements have been undertaken, including tests that are coupled to other methods that use combinations of lifetime and branching ratio measurements [17.3].

The Hook Method

The absorption measurements described above determine the oscillator strength from the line intensity. An alternative absorptive approach is the anomalous dispersion or "hook" method, which determines the oscillator strength from the index of refraction at wavelengths near the edge of an absorption line [17.1]. The advantages of this method are its large dynamic range, its insensitivity to the line shape, and the fact that it does not saturate. The absorbing gas is placed in one arm of an interferometer and a compensator is placed in the other arm. This leads to the formation of oblique interference fringes with two characteristic hooks symmetric about the center of an absorption line. The oscillator strength is determined by the wavelength separation W between the hooks. Defining $K = \lambda_{ik}N_\mathrm{f}$, where N_f is the number of fringes per unit wavelength, then

$$f_{ik} = \frac{\pi K W^2}{\lambda_{ik}^3\alpha^2 a_0 NL} \tag{17.4}$$

where a_0 is the Bohr radius.

Synchrotron Radiation

Storage ring synchrotron radiation facilities now provide a source of continuum radiation that can extend the wavelength range of absorption measurements. A technique [17.4] has been developed and applied that utilizes a hollow cathode discharge as an absorbing sample, synchrotron radiation as a continuum source, and a CCD

Springer Handbook
MS ID: **hb05-b17**
13 June 2005 10:35 CET

array for vacuum ultraviolet (VUV) detection. Here relative oscillator strengths were obtained using two separate detection systems. However, VUV calibration standards are presently lacking (Sect. 17.1.4), and will be required to obtain independent tests (Sect. 17.1.3) of sets of branching fractions.

17.1.2 Emission Measurements

Emission methods use, for example, a hollow cathode, wall-stabilized arc, or shock tube to excite the source. Recent developments in the methods of Fourier transform spectrometry (FTS) [17.5, 6] offer several advantages over grating spectroscopy, as discussed next.

Fourier Transform Spectrometry

As opposed to the dispersive nature of a grating spectrograph, FTS uses interference effects from a Michelson interferometer. All radiation admitted to the spectrometer is thus incident on the detectors at all times, but different wavelengths are distinguished by their spatial modulation frequencies. The interferogram from all sinusoidal signals is sampled at a prescribed interval of path length, and compared with a laser of known frequency following the same optical path. The spectrum is recovered from the interferogram by means of a fast Fourier transform (Sect. 8.1.3). Thus, for an FTS instrument, the spectral range is determined by the sampling step size, whereas the resolution depends on the maximum path difference (this is in contrast to a grating spectrometer where the sampling step determines the resolution, and the scan length determines the spectral range).

The FTS method provides a number of attractive features in precision oscillator strength measurements. The axial symmetry and the replacement of the slit by a larger aperture can provide a throughput that is two orders of magnitude greater than that of a grating instrument of the same resolution. The precision and reproducibility are determined by the laser standard and the linearity of the wavenumber scale. The resolution can be increased as necessary to resolve a specific source line. The superior resolution allows blending and self-absorption to be more readily detected. The spectral range is limited only by detectors and filters. Recently, uv FTS instruments have been constructed that operate from the visible down to 175 nm. Since all wavelengths are observed at all times, errors from drifts in source conditions during scanning are reduced.

Hollow Cathode Lamps

Hollow cathode discharge lamps are used extensively for emission branching fraction measurements [17.5]. These lamps can generate an emission spectrum of essentially any element, and the relatively low collision rates result in line profiles that are narrow and primarily Doppler broadened. The narrow line width is a major advantage when studying line-rich spectra. The low collision rates also imply that the discharges are far from local thermodynamic equilibrium (LTE). However, this does not affect the determination of branching fractions, where only the relative strengths of lines from a common upper level are measured. These measurements can then be put on an absolute basis if lifetime measurements are available for all of the upper levels.

17.1.3 Combined Absorption, Emission and Lifetime Measurements

By combining measurements obtained in emission with those obtained in absorption (or dispersion) to obtain branching ratios, and then incorporating lifetime measurements, it is possible to use a scheme that requires no knowledge of level populations [17.1]. The scheme was originally proposed by Ladenburg in 1933, and its various modern implementations are known as "leap-frogging," "linkage" and "bow ties".

The principle of "leap-frogging" or "linkage" is illustrated in Fig. 17.1a. The decay of level 1 is unbranched, so the $1 \rightarrow 2$ transition rate is assumed known (kn) from a lifetime measurement. This is used to specify the $2 \rightarrow 3$ oscillator strength using relative absorption (ab) measurements for the $2 \rightarrow 1 : 2 \rightarrow 3$ oscillator strength ratio (and appropriate factors of the wavelengths and degeneracies). In a similar manner, this is subsequently combined with relative emission (em) measurements of the $3 \rightarrow 2 : 3 \rightarrow 4$ branching ratio to determine the $3 \rightarrow 4$ transition rate.

The principle of "bow ties" is illustrated in Fig. 17.1b. The two branching ratios for $1 \rightarrow 2 : 1 \rightarrow 4$ and for $3 \rightarrow 2 : 3 \rightarrow 4$ are measured in emission (em). The two oscillator strength ratios for $2 \rightarrow 1 : 2 \rightarrow 3$ and for $4 \rightarrow 1 : 4 \rightarrow 3$ are measured in absorption (ab). After correction for wavelength and degeneracy factors between f and A values, these relationships are combined into a quantity known as the "bow tie ratio," which would be unity for ideally accurate measurements. A significant deviation from unity can be used to trace the observations that are in error. Figure 17.1b is a "simple bow tie" connecting two upper and two lower levels with four transitions. Higher order sets of measurements can

Springer Handbook
MS ID: **hb05-b17**
13 June 2005 10:35 CET

oscillator strength!measurement of
highly stripped ions
branching ratio!radiative
branching ratio!in highly ionized atoms
krypton, one-electron
radiative lifetime

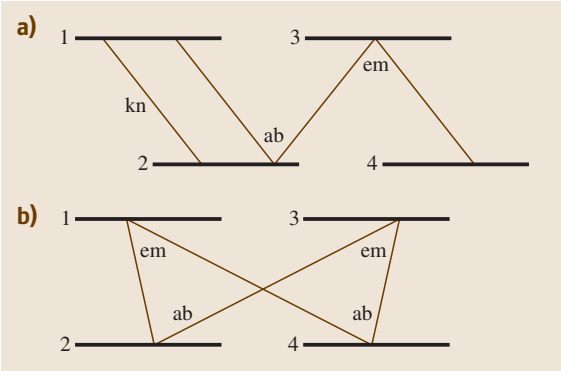

Fig. 17.1a,b Illustration of methods for the determination of ratios of oscillator strengths (ab = absorption, em = emission, kn = known)

be similarly coupled; for example, a set of transitions between three lower levels and three upper levels can be coupled by nine simple bow ties.

In cases where both lifetime and complete branching ratio measurements exist for the same upper level, then the branching ratios can be normalized to branching fractions divided by the lifetime to obtain absolute transition probabilities.

17.1.4 Branching Ratios in Highly Ionized Atoms

In highly ionized atoms, many measurements of lifetimes in the 1–5% accuracy range have been made by ANDC (Sect. 17.2.2) analysis of beam–foil measurements. However, little work exists for the precision measurement of branching ratios in highly ionized atoms, where an intensity calibrationof the detection equipment is particularly difficult. In beam—foil excitation, for example, Doppler broadening and Doppler shifts, polarization due to anisotropic excitation, and the short wavelength (≤ 200 nm) nature of the radiation are not well-suited for use with standard techniques for calibrating grating spectrometer and detection systems by the use of calibrated lamps. Calibrations have been carried out using synchrotron radiation, or through the use of previously known branching ratios.

One way in which lifetime measurements are used to determine branching ratios involves precision studies of the lifetimes of the individual fine structure components of a multiplet decay. If one fine structure level has a decay channel that is not available to the other levels (for example, spin-changing transition or an autoionization mode made possible by a J-dependent intermediate coupling) then the transition rate of the extra channel can be determined by differential lifetime measurements.

The use of Si(Li) detectors in the measurement of very short wavelength radiation in highly ionized atoms also offers possibilities for branching ratio measurements. Since these devices can specify the photon energy from pulse height information without the need for a spectrometer, they can be calibrated for detection efficiency as a function of energy. This type of detection was recently used to determine the branching ratio of the magnetic dipole channel to the two-photon decay channel in the 2s $2S_{\frac{1}{2}}$ state in one-electron krypton [17.7].

Although radiometric calibration standards are available for $\lambda > 280$ nm, technical challenges exist for their extension to shorter wavelengths. The urgent need for these standards and their desired characteristics have been discussed by *Lawler* et al. [17.4], and an operational prescription for combining sources of uncertainty in their specification has been presented by *Sikström* et al. [17.8]. A semi-empirical method for obtaining line intensity standards in the VUV has also been proposed [17.9, 10] that uses intermediate coupling (IC) amplitudes deduced from measured energy level data to obtain intensity ratios. This utilizes the observation that the ns^2np^2 and $ns^2np(n+1)s$ configurations in the Si, Ge and Sn isoelectronic sequences exhibit negligible configuration interaction, hence the intensity ratios within their transition arrays are accurately prescribed by the IC amplitudes. For the neutral atoms the transitions occur in the visible region, and measurements confirm the validity of the empirical values. Thus, isoelectronic extensions can yield VUV standards.

17.2 Lifetimes

The total transition rate summed over all decay channels can be measured either through frequency-resolved studies of the level width, or through time-resolved studies of the level lifetime. In order to determine the natural linewidth in a field-free spectroscopic measurement, either the lifetime must be very short, or the Doppler, pressure, and instrumental broadenings must be made very small. Line widths have been de-

Springer Handbook
MS ID: **hb05-b17**
13 June 2005 10:35 CET

termined using Fabry–Perot spectrometry at very low temperatures and pressures, and in beam–foil studies of radiative transitions in which the lower level decays very rapidly via autoionization. The linewidth can also be determined through the use of the phase shift method. Here modulated excitation is applied to the source, thus producing similarly modulated emitted radiation, and the width can be specified from the phase shift between the two signals. Other methods involve resonance fluorescence techniques, where sub-Doppler widths are obtained because the width of the exciting radiation selects a subset of particle motions within the sample. Resonance fluorescence techniques that can be used to determine level widths include zero-field level crossing (the Hanle effect), high-field level crossing, and double optical resonance methods, but the Hanle effect is the most common.

17.2.1 The Hanle Effect

In its most commonly used form, the Hanle effect makes use of polarized resonance radiation to excite atoms in the presence of a known variable magnetic field. The magnetic substates of the sample are anisotropically excited, and the subsequent radiation possesses a preferred angular distribution. By applying the magnetic field in a direction perpendicular to the anisotropy, the angular distribution is made to precess, producing oscillations in the radiation observed at a fixed angle. At infinite precessional frequency the intensity would be proportional to the instantaneous average angular intensity, but at finite precessional frequency it depends upon the decay that has occurred during each quarter rotation. Measured as a function of magnetic field, the emitted intensity has a Lorentzian shape centered about zero field with a width that depends on the lifetime and g-factor of the level [17.2].

17.2.2 Time-Resolved Decay Measurements

The most direct method for the experimental determination of level lifetimes is through the time-resolved measurement of the free decay of the fluorescence radiation following a cutoff of the source of excitation. An important factor limiting the accuracy is the repopulation of the level of interest by cascade transitions from higher-lying levels. For this reason, decay curve measurements fall into two classes: those that involve selective excitation of the level of interest, thus eliminating cascading altogether; and those that use correlations between cascade connected decays to account for the effects of cascades.

Selective Excitation

Lifetime measurements accurate to within a few parts in 10^3 have been obtained through selective excitation produced when appropriately tuned laser light is incident on a gas cell or a thermal beam, or on a fast ion beam (Sect. 18.1). With a gas cell or thermal beam, the timing is obtained by a pulsed laser and delayed coincidence detection. With a fast ion beam, time-of-flight methods are used. In either case, after removal of the background, the decay curve of intensity vs. time is a single exponential, and the lifetime is obtained from its semilogarithmic slope. Laser-excited time-of-flight studies were first carried out by observing the optical decay of the ion in flight following excitation using a laser beam which crossed the ion beam. In these studies, the laser light was tuned to the frequency of the desired absorption transition either through the use of a tunable dye laser, or by varying the angle of intersection to exploit the Doppler effect. Recent measurements have utilized diode laser excitation in this geometry [17.11]. A number of adaptations of this technique have been developed in which the laser and ion beams are made to be collinear, and are switched into and out of resonance within a segment of the beam by use of the Doppler effect [17.12]. The collinear geometry can provide a longer excitation region and less scattering of laser light into the detector than occurs in the crossed beam geometry. In one adaptation [17.13], excitation occurs within an electrostatic velocity switch, and the time resolution is obtained by physically moving the velocity switch. In another adaptation [17.12], the ion beam is accelerated with a spatially varying voltage ramp. The resonance region is moved relative to a fixed detector by time-sweeping either the laser tuning or the ramp voltage.

While these selective excitation methods totally eliminate the effects of cascade repopulation, they are generally limited to levels in neutral and singly ionized atoms that can be accessed from the ground state by strongly absorptive E1 transitions, and the selectivity itself is a limitation. Many very precise measurements have been made by these techniques, but they have primarily involved $\Delta n = 0$ resonance transitions in neutral alkali atoms and singly ionized alkali-like ions. A summary of these measurements is given in Table 17.1, and a comparison

Springer Handbook
MS ID: **hb05-b17**
13 June 2005 10:35 CET

Table 17.1 Measured $np\ ^2P_J$ lifetimes

Atom	n	J	τ (ns)
Li	2	1/2	27.20(20)[a], 27.29(4)[b]
Na	3	1/2	16.38(8)[c], 16.40(3)[b], 16.30(2)[d]
	3	3/2	16.36(2)[c], 16.25(2)[d]
Mg^+	3	1/2	3.854(30)[d]
	3	3/2	3.810(40)[e]
Ca^+	4	1/2	7.07(7)[f], 7.098(20)[g]
	4	3/2	6.87(6)[f], 6.924(19)[g]
Cu	4	1/2	7.27(6)[h]
	4	3/2	7.17(6)[h]
Sr^+	5	1/2	7.47(7)[i]
	5	3/2	6.69(7)[i]
Ag	5	1/2	7.408(32)[j]
	5	3/2	6.791(19)[j]
Cd^+	5	1/2	3.11(3)[k]
	5	3/2	2.77(6)[k]
Cs	6	3/2	30.55(27)[l]
Ba^+	6	1/2	7.92(8)[i]
	6	3/2	6.312(16)[m]

[a][17.15] [b][17.16] [c][17.17] [d][17.18]
[e][17.19] [f][17.20] [g][17.21] [h][17.22]
[i][17.23] [j][17.24] [k][17.25] [l][17.11]
[m][17.26]

of these values with theoretical calculations is given in [17.14].

Advances have recently been made in the measurement of transition probabilities of long-lived metastable levels. Through a laser probing technique [17.27] using an ion storage ring, an extremely long lifetime (28 s) has been measured [17.28]. The metastable level is populated in the ion source and preserved in the storage ring until it is destructively probed at variable times after excitation. The laser light is collinearly merged with the beam and tuned to a transition that promotes the population of the metastable level to a higher unstable level. The fluorescence subsequently emitted by this unstable level gives a relative measure of the population of the metastable level. Thus, by varying the delay time between the excitation and the laser probing, a decay curve of the population remaining is obtained.

Nonselective Excitation

Much more general access can be obtained by nonselective excitation methods, such as pulsed electron beam bombardment of a gas cell or gas jet, or in-flight excitation of a fast ion beam by a thin foil. Pulsed electron beam excitation can be achieved either through use of a suppressor grid, or by repetitive high frequency deflection of the beam across a slit so as to chop the beam. Particularly in the case of weak lines, the high frequency deflection technique offers the advantages of high current and sharp cut-off times. The high currents yield high light levels, so that high resolution spectroscopic methods can be used to eliminate the effects of line blending. Pulsed electron excitation methods are well suited to measurements in neutral and near neutral ions (although for very long lifetimes in ionized species, the decay curves can be distorted if particles escape from the viewing volume through the Coulomb explosion effect [17.29]). However, for highly ionized atoms, the only generally applicable method is thin foil excitation of a fast ion beam. Nonselective excitation techniques can also be applied to measurements such as the phase shift method [17.30] and the Hanle effect [17.31], in which case cascade repopulation also can become a serious problem. However, most of the attempts to eliminate or account for cascade effects have occurred in decay curve studies.

In beam–foil studies, the excitation is created in the dense solid environment of the foil, after which the ions emerge into a field free, collision free, high vacuum region downstream from the foil. A time-resolved decay curve is obtained by translating the foil upstream or downstream relative to the detection apparatus. The beam is a very tenuous plasma, which has both advantages and disadvantages. The low density avoids the effects of collisional de-excitation and radiation trapping, but also produces relatively low light levels. This requires fast optical systems with a corresponding reduction in wavelength dispersion, and care must be taken to avoid blending of these Doppler broadened lines. Methods have been developed by which grating monochromators can be refocussed to a moving light source, thus utilizing the angular dependence of the Doppler effect to narrow and enhance the lines.

In these nonselective excitation methods, the decay curve involves a sum of many exponentials, one corresponding to the primary level, and one to each level that cascades (either directly or indirectly) into it. Decay exponentials do not comprise an orthogonal set of functions, and the representation of an infinite sum by a finite sum through curve fitting methods (Sect. 8.1.2) can lead to large errors. Fortunately, alternative methods to exponential curve fitting exist, which permit the ac-

Springer Handbook
MS ID: **hb05-b17**
13 June 2005 10:35 CET

curate extraction of lifetimes to be made from correlated sets of nonselectively populated decay curves.

ANDC Method

Precision lifetime values have been extracted from cascade-affected decay curves by a technique known as the arbitrarily normalized decay curve (ANDC) method (Sect. 18.1.1, [17.32]), which exploits dynamical correlations among the cascade-related decay curves. These correlations arise from the rate equation that connects the population of a given level to those of the levels that cascade directly into it. The instantaneous population of each level n is, to within constant factors ξ_n involving the transition probabilities and detection efficiencies, proportional to the intensity of radiation $I_n(t)$ emitted in any convenient decay branch. In terms of these intensities, the population equation for the level n can be written in terms of its direct cascades from levels i as

$$\frac{\mathrm{d}I_n}{\mathrm{d}t}(t_\mathrm{p}) = \sum_i \xi_i I_i(t_\mathrm{p}) - I_n(t_\mathrm{p})/\tau_n \,. \qquad (17.5)$$

Thus, if all decay curves are measured at the same discrete intervals of time t_p, the population equation provides a separate independent linear relationship among these measured decay curves for each value of t_p, with common constant coefficients given by the lifetime τ_n and the normalization parameters ξ_i. Although the sum over cascades is formally unbounded, the dominant effects of cascading from highly excited states are often accounted for by indirect cascading through the lower states, in which case the sum can be truncated after only a few terms. ANDC analysis consists of using this equation to relate the measured $I_k(t_\mathrm{p})$ (using numerical differentiation or integration) to determine τ_k and the ξ_i through a linear regression. If all significant direct cascades have been included, the goodness-of-fit will be uniform for all time subregions, indicating reliability. If important cascades have been omitted or blends are present, the fit will vary over time subregions, indicating a failure of the analysis. Very rugged algorithms have been developed [17.33] that permit accurate lifetimes to be extracted even in cases where statistical fluctuations are substantial, and studies of the propagation and correlation of errors have been made. Clearly the ANDC method is most easily applied to systems for which repopulation effects are dominated by a small number of cascade channels. Further applications are discussed in Sect. 18.1.1.

17.2.3 Other Methods

Coincidence measurements provide another method for elimination of cascade effects. While the low count rates and correspondingly high accidental rates make the application of these methods difficult for optical spectra, the use of Si(Li) for the very short wavelength emission in very highly ionized systems offers new possibilities [17.34] for these measurements.

Another method of accounting for cascading involves the combined use ofa laser and beam–foil excitation [17.35,36]. The beam–foil excitation provides a source of ions in excited states, and a chopped laser is used to stimulate transitions between two excited states. By subtracting the decay curves obtained with laser on and with laser off, the cascade-free, laser-produced portion of the decay curve is obtained.

17.2.4 Multiplexed Detection

Recently, the detection efficiency and reliability of beam–foil measurements have been improved through the use of position sensitive detectors (PSD), which permits measurement of decay curves as a function both of wavelength and of time since excitation. The PSD is mounted at the exit focus of the analyzing monochromator, where it records all lines within a given wavelength interval simultaneously, including reference lines with the same Doppler shifts. Decay curves can be constructed by integrating over a line profile, and that profile can be examined for exponential content to eliminate blending. The time dependent backgrounds underlying the decay curves are directly available from the neighboring channels.

The use of multiplexed detection greatly enhances the data collection efficiency, and causes many possible systematic errors to cancel in differential measurements. Effects such as fluctuations in the beam current, degradation of the foil, divergence of the beam, etc., affect all decay curves in the same way.

The most accurate measurement [17.37] made by beam–foil excitation ($\pm 0.26\%$) used a type of multiplexed detection in which two spectrometers simultaneously viewed the decays of the $1P_1$ and $3P_1$ levels of the 1s3p configuration in neutral helium. The $1P_1$ emission exhibited the desired multi-exponential decay curve (with only weak cascading), whereas the $3P_1$ emission exhibited a zero field quantum beat pattern

Springer Handbook
MS ID: **hb05-b17**
13 June 2005 10:35 CET

superimposed on its decay because of the anisotropic excitation of that level. The quantum beats provided an in-beam time base calibration which permitted this high precision.

References

17.1 M. C. E. Huber, R. J. Sandeman: Rep. Prog. Phys. **49**, 397 (1986)
17.2 L. J. Curtis: *Atomic Structure and Lifetimes: A Conceptual Approach* (Cambridge Univ. Press, Cambridge 2003)
17.3 D. E. Blackwell: *Atomic Spectra and Oscillator Strengths for Astrophysics and Fusion Research*, ed. by J. E. Hansen (North-Holland, Amsterdam 1990) p. 160
17.4 J. E. Lawler, S. D. Bergeson, J. A. Feldchak, K. L. Mullman: Phys. Scr. **T83**, 11 (1999)
17.5 J. E. Lawler, S. D. Bergeson, R. C. Wamsley: Phys. Scr. **T47**, 29 (1993)
17.6 A. Thorne, U. Litzén, S. Johansson: *Spectrophysics: Principles and Applications* (Springer, Berlin, Heidelberg 1999)
17.7 S. Cheng, H. G. Berry, R. W. Dunford, D. S. Gemmell, E. P. Kanter, B. J. Zabransky, A. E. Livingston, L. J. Curtis, J. Bailey, J. A. Nolen Jr.: Phys. Rev. A **47**, 903 (1993)
17.8 C. M. Sikström, H. Nilsson, U. Litzén, H. Lundberg: J. Quant. Spectrosc. Radiat. Transfer **74**, 355 (2002)
17.9 L. J. Curtis: J. Phys. B **31**, L769 (1998)
17.10 L. J. Curtis: J. Phys. B **33**, L259 (2000)
17.11 C. E. Tanner, A. E. Livingston, R. J. Rafac, F. G. Serpa, K. W. Kukla, H. G. Berry, L. Young, C. A. Kurtz: Phys. Rev. Lett. **69**, 2765 (1992)
17.12 J. Jin, D. A. Church: Phys. Rev. **47**, 132 (1993)
17.13 H. Winter, M. L. Gaillard: Z. Phys. **A281**, 311 (1977)
17.14 L. J. Curtis: Phys. Scr. **48**, 599 (1992)
17.15 J. Carlsson, L. Sturesson: Z. Phys. **D14**, 281 (1989)
17.16 A. Gaupp, P. Kuske, H. J. Andrä: Phys. Rev. A **26**, 3351 (1982)
17.17 J. Carlsson: Z. Phys. **D9**, 147 (1988)
17.18 U. Volz, M. Majerus, H. Liebel, A. Schmitt, H. Schmoranzer: Phys. Rev. Lett. **76**, 2862 (1996)
17.19 W. Ansbacher, Y. Li, E. H. Pinnington: Phys. Lett. A **139**, 165 (1989)
17.20 R. N. Gosselin, E. H. Pinnington, W. Ansbacher: Nucl. Instrum. Meth. Phys. Res. **B31**, 305 (1988)
17.21 J. Jin, D. A. Church: Phys. Rev. Lett. **70**, 3213 (1993)
17.22 J. Carlsson, L. Sturesson, S. Svanberg: Z. Phys. **D11**, 287 (1989)
17.23 P. Kuske, N. Kirchner, W. Wittmann, H. J. Andrä, D. Kaiser: Phys. Lett. A **64**, 377 (1978)
17.24 J. Carlsson, P. Jönsson, L. Sturesson: Z. Phys. **D16**, 87 (1990)
17.25 E. H. Pinnington, J. J. van Hunen, R. N. Gosselin, B. Guo, R. W. Berends: Phys. Scr. **49**, 331 (1994)
17.26 H. J. Andrä: *Beam–Foil Spectroscopy*, Vol. 2, ed. by I. A. Sellin, D. J. Pegg (Plenum, New York 1976) p. 835
17.27 J. Lidberg, A. Al-Kahlili, L. O. Norlin, P. Royen, X. Tordoir, S. Mannervik: Nucl. Instrum. Meth. Phys. Res. B **152**, 157 (1999)
17.28 H. Hartman, D. Rostohar, A. Derkatch, P. Lundin, P. Schef, S. Johansson, H. Lundberg, S. Mannervik, L.-O. Norlin, P. Royan: J. Phys. B **36**, L197 (2003)
17.29 L. J. Curtis, P. Erman: J. Opt. Soc. Am. **67**, 1218 (1977)
17.30 L. J. Curtis, W. H. Smith: Phys. Rev. A **9**, 1537 (1974)
17.31 M. Dufay: Nucl. Instrum. Meth. **110**, 79 (1973)
17.32 L. J. Curtis: *Beam–Foil Spectroscopy*, ed. by S. Bashkin (Springer, Berlin, Heidelberg 1976) p. 3
17.33 L. Engström: Nucl. Instrum. Meth. **202**, 369 (1982)
17.34 R. W. Dunford, H. G. Berry, S. Cheng, E. P. Kanter, C. Kurtz, B. J. Zabransky, A. E. Livingston, L. J. Curtis: Phys. Rev. A **48**, 1929 (1993)
17.35 H. Harde, G. Guthöhrlein: Phys. Rev. A **10**, 1488 (1974)
17.36 Y. Baudinet-Robinet, H.-P. Garnir, P.-D. Dumont, J. Résimont: Phys. Rev. A **42**, 1080 (1990)
17.37 G. Astner, L. J. Curtis, L. Liljeby, S. Mannervik, I. Martinson: Z. Phys. **279**, 1 (1976)

Springer Handbook
MS ID: **hb05-b17**
13 June 2005 10:35 CET